### Title

Dissolving Microneedle Delivery of a Prophylactic HPV Vaccine




### Journal

Biomacromolecules, 23(3)

### ISSN

1525-7797



### Authors

Ray, Sayoni
Wirth, David M
Ortega-Rivera, Oscar A
et al.



### Publication Date

2022-03-14

### DOI

10.1021/acs.biomac.1c01345

Peer reviewed

HHS Public Access

Author manuscript

*Biomacromolecules*. Author manuscript; available in PMC 2023 January 10.

Published in final edited form as:

*Biomacromolecules*. 2022 March 14; 23(3): 903–912. doi:10.1021/acs.biomac.1c01345.

# Dissolving Microneedle Delivery of a Prophylactic HPV Vaccine

**Sayoni Ray**,
Department of NanoEngineering and Center for Nano-ImmunoEngineering, University of California-San Diego, La Jolla, California 92039, United States

**David M. Wirth**,
Department of NanoEngineering, University of California-San Diego, La Jolla, California 92039, United States

**Oscar A. Ortega-Rivera**,
Department of NanoEngineering and Center for Nano-ImmunoEngineering, University of California-San Diego, La Jolla, California 92039, United States

**Nicole F. Steinmetz**,
Department of NanoEngineering, Center for Nano-ImmunoEngineering, Institute for Materials Discovery and Design, Department of Bioengineering, Department of Radiology, and Moores Cancer Center, University of California-San Diego, La Jolla, California 92039, United States

**Jonathan K. Pokorski**
Department of NanoEngineering, Center for Nano-ImmunoEngineering, and Institute for Materials Discovery and Design, University of California-San Diego, La Jolla, California 92039, United States

## Abstract

Prophylactic vaccines capable of preventing human papillomavirus (HPV) infections are still inaccessible to a vast majority of the global population due to their high cost and challenges related to multiple administrations performed in a medical setting. In an effort to improve distribution and administration, we have developed dissolvable microneedles loaded with a thermally stable HPV vaccine candidate consisting of Q$\beta$ virus-like particles (VLPs) displaying a highly conserved epitope from the L2 protein of HPV (Q$\beta$-HPV). Polymeric microneedle delivery of Q$\beta$-HPV produces similar amounts of anti-HPV16 L2 IgG antibodies compared to traditional subcutaneous injection while delivering a much smaller amount of intradermal dose. However, a dose sparing effect was found. Furthermore, immunization yielded neutralizing

**Corresponding Authors Nicole F. Steinmetz** – Department of NanoEngineering, Center for Nano-ImmunoEngineering, Institute for Materials Discovery and Design, Department of Bioengineering, Department of Radiology, and Moores Cancer Center, University of California-San Diego, La Jolla, California 92039, United States; nsteinmetz@ucsd.edu; **Jonathan K. Pokorski** – Department of NanoEngineering, Center for Nano-ImmunoEngineering, and Institute for Materials Discovery and Design, University of California-San Diego, La Jolla, California 92039, United States; jpokorski@ucsd.edu.

Supporting Information

The Supporting Information is available free of charge at https://pubs.acs.org/doi/10.1021/acs.biomac.1c01345.
Expression and characterization of Q$\beta$-HPV via genetic recombination, microneedle preparation schematic and application, and calculation of dose sparing and amplification effects (PDF)

The authors declare the following competing financial interest(s): JKP and NFS are co-founders of Mosaic ImmunoEngineering Inc. who has interest in this technology.

antibody responses in a HPV pseudovirus assay. The vaccine candidate was confirmed to be stable at room temperature after storage for several months, potentially mitigating many of the challenges associated with cold-chain distribution. The ease of self-administration and minimal invasiveness of such microneedle patch vaccines may enable wide-scale distribution of the HPV vaccine and lead to higher patient compliance. The Q$\beta$ VLP and its delivery technology is a plug-and-play system that could serve as a universal platform with a broad range of applications. Q$\beta$ VLPs may be stockpiled for conjugation to a wide range of epitopes, which are then packaged and delivered directly to the patient via noninvasive microneedle patches. Such a system paves the way for rapid distribution and self-administration of vaccines.

## Graphical Abtract

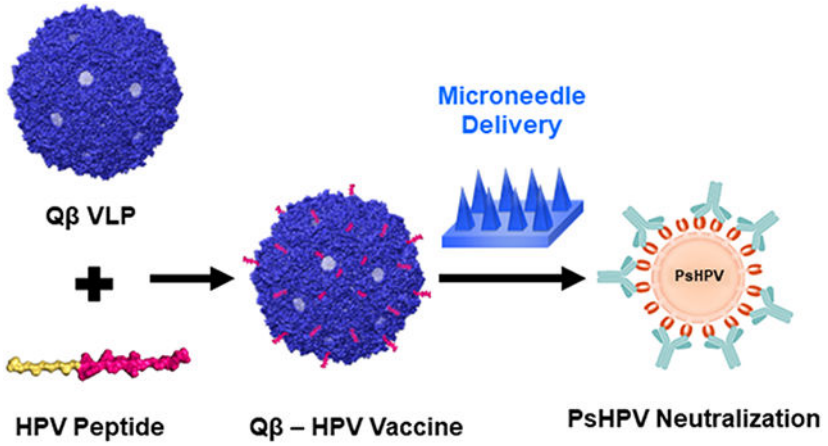


## 1. INTRODUCTION

The human papillomavirus (HPV) is a prevalent sexually transmitted infection, accounting for ~5% of all human cancers including most of the cervical malignancy, penile, vulvar, anal, vaginal, and oropharyngeal carcinoma worldwide.[1,2] Among them, cervical cancer is the fourth-most frequent cancer among women, affecting over half a million women every year with a high mortality rate of 50%.[3] Over 90% of cervical cancer cases are caused by HPV, and, unlike other malignancies, the disease usually claims the lives of comparatively younger women aged 40–50 years.[2-4] HPV is also responsible for head and neck cancers and over 40% of the oropharyngeal cancers, claiming approximately another 120 000 lives annually.[2] Recently, prophylactic HPV vaccines were licensed; however, several challenges still remain. The high cost of the vaccine is an impediment to distribution in the developing world, and the patient's hesitancy to undergo a multi-injection vaccine regimen continues to limit uptake. Approved HPV vaccines require three doses within a period of 6 months for adults (above 15 years) and two doses within a period of 6–12 months for children between 9 and 14 years. Thus, the procedure demands multiple visits to health-care centers, resulting in poor patient compliance and subsequent vaccine wastage.[5,6] In the United States, only about 50% of the eligible population completes the full vaccination schedule. Further challenges arise with delivering such a vaccine to developing countries where the lack of effective cold-chain transportation and storage, as well as a shortage

of trained health-care professionals, places additional burdens on vaccine distribution.[5,7-9] Despite the development of a safe and effective prophylactic HPV vaccine, it remains unlikely to eradicate HPV without a more advanced delivery system to enable global mass vaccination.[8-11]

One way to address these drawbacks would be the implementation of dissolvable microneedle patches to deliver a prophylactic HPV vaccine candidate. Microneedles enable self-administration, reduce needle-phobia, decrease the chances of infection from the injection site, and reduce the demand for trained health-care professionals.[12-14] Microneedles can be as effective as traditional injection since they inherently target densely populated antigen presenting cells (APCs) in the skin.[15,16] Microneedle technology is an ideal approach for a rapid mass vaccination program.[17]

In this work, we have developed an adaptable dissolving polymer microneedle-based platform using a HPV vaccine formulation derived from virus-like particles (VLPs),[18-22] specifically the capsid protein of the highly stable and immunogenic bacteriophage Q$\beta$.[23-26] Our prophylactic HPV vaccine candidate was synthesized by conjugating a conserved region from the high-risk HPV16 L2 peptide[27,28] onto the surface of Q$\beta$[29]. While commercial vaccines are now utilizing the major capsid protein L1 of HPV in their formulation, minor capsid protein L2 has shown promising results to cross-neutralize diverse types of HPVs due to its conserved sequence and holds potential for a next-generation universal HPV vaccine.[27] The $L2_{17–31}$ epitope is a good candidate because this epitope is transiently exposed to the virus surface and the sequence is conserved among different HPV strains; others have reported success in preclinical work.[27,30-32] Herein, we report the creation of HPV microneedle vaccination devices, their long-term stability, and the resulting protective antibody formation following administration.

## 2. MATERIALS AND METHODS

### 2.1. VLP Production.

Q$\beta$ VLPs[33-35] were expressed in *Escherichia coli* using the coat protein sequence from bacteriophage Q$\beta$, purified (characterization details are shown in Figure S1), and conjugated to HPV peptides to produce Q$\beta$-HPV VLPs as previously described.[29] In short, 28 mg of Q$\beta$ particles was reacted with 1250-fold molar equivalents per particle of $SM(PEG)_8$ (Thermo Fisher Scientific) in ~2 mL of phosphate-buffered saline (PBS) (Fisher Scientific) at room temperature for 1.5 h (pH 7.4). The excess linker molecules were removed by filtration through a 100 kDa centrifugal cutoff filter (Thermo Fisher Scientific) at 3000*g* for 15 min and washed twice with PBS. The concentrated solution was resuspended in ~2 mL of PBS and mixed with the 1250-fold molar equivalents (per Q$\beta$ particle) of $L2_{17–31}$ peptides (GenScript; Figure 1A) at room temperature for 2.5 h to complete the reaction. Q$\beta$-HPV VLPs were purified by a 100 kDa centrifugal filter at 3000*g* for 15 min and washed twice with PBS. The VLPs were further purified by dialyzing for 2 days against PBS at 4 °C and then stored at 4 °C until their use in later process steps.

### 2.2. Qβ-Alexa VLP Bioconjugation.

Qβ was labeled with AlexaFluor-488 dye by the reaction of 8 mg of Qβ-VLP with 1250-fold molar equivalents of AlexaFluor-488 NHS-ester (Lumiprobe) per Qβ particle in 1 mL of 0.01 M potassium phosphate ($K_2HPO_4$ and $KH_2PO_4$, pH 8.3) buffer solution for 4 h at room temperature in a rotisserie shaker. The excess dye was removed using a 100 kDa MWCO centrifugal filter (Thermo Fisher Scientific) by centrifugation at 3000*g* for 15 min at 4 °C, followed by washing twice with PBS. The Qβ-Alexa VLPs were pelleted by ultracentrifugation at 52 000 rpm (TLA 55, fixed angle rotor, Beckman Coulter) for 1 h at 4 °C and resuspended in PBS at pH 7.4. The purified Qβ-Alexa VLPs were collected after dialyzing for 24 h against PBS at 4 °C and stored at 4 °C.

### 2.3. Characterization of VLPs.

The concentration of VLPs was measured using a Pierce BCA assay kit (Thermo Fisher Scientific) as per the manufacturer's protocols. VLPs were characterized by sodium dodecyl sulfate-polyacrylamide gel electrophoresis (SDS-PAGE), fast protein liquid chromatography (FPLC), dynamic light scattering (DLS), and transmission electron microscopy (TEM). SDS-PAGE was carried out using NuPAGE 12% Bis–Tris protein gels (Thermo Fisher Scientific) for 37 min at 200 V. Images were acquired using the FluorChem R imaging system (ProteinSimple) after staining the gel with Coomassie Brilliant Blue (Fisher Scientific). FPLC was performed using 300 μL of ~1 mg/mL VLP solution by an AKTA-FPLC 900 system fitted with the Superose 6 Increase 10/300 GL columns (GE Healthcare); PBS (pH 7.4) served as the mobile phase at a flow rate of 0.4 mL/min. DLS measurements were done with 100 μL of 0.1 mg/mL VLP solution using a Malvern Instruments Zetasizer Nano at 25 °C in plastic disposal cuvettes. The size was calculated from the weighted average of the number distribution. TEM was performed on an FEI Tecnai Spirit G2 Bio TWIN transmission electron microscope. The samples were prepared by mounting 0.2 mg/mL VLPs on the 400-mesh hexagonal copper grids and stained with 2% (w/v) uranyl acetate.

### 2.4. Microneedle Preparation.

The poly(vinylpyrrolidone) (PVP) microneedles were prepared (shown in Figure S2) using poly(dimethylsiloxane) (PDMS) molds (Micropoint Technologies) with an 8 mm × 8 mm square patch containing 10 × 10 arrays of pyramidal needles with a height of 675 μm and a base length of 200 μm. The VLPs were loaded onto it following the procedure as described here. At first, a 10 μL of aliphatic release agent (1 part light mineral oil in 20 parts hexane v/v) was added to the PDMS molds and the mixture was allowed to air-dry for 1 min to allow the volatiles to evaporate. The VLPs were suspended in deionized water by buffer exchange; prior to the microneedle preparation, the Qβ VLPs were mixed with PVP (40 kDa) (VWR), at a concentration defined in the text, to prepare an aqueous solution with a final PVP concentration of 500 mg/mL. Approximately, 75 μL of the PVP solution was added to the molds, and the samples were placed in flat-bottom 50 mL falcon tubes. The falcon tubes were centrifuged in a bucket wheel centrifuge (Eppendorf 5804) for 90 min at 40 °C. It was important to place the tubes only in the center holes of each bucket to avoid off-axis acceleration, which would cause the PVP solution to spill out during centrifugation.

The PDMS microneedle molds with centrifuged PVP were desiccated over $CaCl_2$ overnight at room temperature. Afterward, a backing layer was added by filling the headspace of the PDMS molds to the brim with ~10 to 20 μL of Anycubic 405 nm Translucent Green UV Resin and were placed under a lab-made 15 mW/cm$^2$ 405 nm UV light source for 60 s to cure the resin. The microneedle patches were then demolded from the PDMS molds using tweezers and placed in a desiccator over calcium chloride for storage.

### 2.5. Microneedle Characterization.

The microneedles were sputter-coated with gold using a Pelco SC-7 Auto Sputter Coating system. The samples were then imaged under an FEI Quanta 600 scanning electron microscope (SEM). To characterize the purity and activity of VLPs after loading into the microneedles, a microneedle extract was prepared by dissolving the patches in PBS and characterizing the released VLPs using the methods listed above. Polymer removal was done using Amicon ultracentrifugal filter units (EMD Millipore), as required for characterization.

To determine the penetration efficiency of the microneedles, pigskin was purchased from a local grocer and microneedles loaded with Qβ-Alexa were inserted into a spring applicator and held against the skin for 2 min after spring-assisted application. The top view and cross section of the skin were visualized under a fluorescence microscope (EVOS).

### 2.6. Immunization.

All animal work was performed according to the approved protocol by the Institutional Animal Care and Use Committee (IACUC), University of California, San Diego (UCSD). Female Balb/c mice (6–8 weeks) were purchased from Jackson Laboratory and immunized twice (prime and boost) at an interval of 3 weeks. The following groups of mice were immunized: (1) microneedles loaded with 100 μg of Qβ-HPV VLPs ($n$ = 8); (2) microneedles loaded with 500 μg of Qβ-HPV VLPs ($n$ = 8); (3) subcutaneous injection of 100 μg of Qβ-HPV VLPs ($n$ = 4); (4) subcutaneous injection of 1.5 μg of Qβ-HPV VLPs ($n$ = 5); and (5) empty microneedles ($n$ = 4). In all of the cases, the microneedles were applied on the back of the shaved mice using a spring applicator (Micropoint Technologies) and taped overnight with a bandage. Blood was collected by retro-orbital bleeding on weeks 0, 2, 5, and 7 of the experiment, and the plasma was separated by centrifugation at 2000$g$ for 5 min. The mice plasma was preserved at −80 °C for further experiments.

### 2.7. Determination of Antibody Titers.

IgG antibody titers were determined using enzyme-linked immunosorbent (ELISA) and Pierce maleimide activated plates (Thermo Fisher Scientific). Plates were washed three times with 200 μL of wash buffer (PBS with 0.1% (v/v) Tween 20) (Fisher Scientific). The plates were coated with 100 μL of HPV peptide (10 μg/mL) per well prepared in a binding buffer (0.1 M sodium phosphate, 0.15 M sodium chloride, 10 mM EDTA, pH 7.2) (Fisher Scientific) and incubated overnight at 4 °C in a plate shaker. The plates were washed three times using 200 μL of wash buffer for each wash. A freshly prepared cysteine (Fisher Scientific) solution (10 μg/mL) in binding buffer was added to each well (200 μL/well), and the plates were incubated for 1 h at room temperature in a plate shaker (400 rpm). The wells were again washed three times (200 μL/well) with a wash buffer. The 2-fold serially diluted

mice plasma (diluted in binding buffer) was added to the wells (100 μL/well) and incubated for 1 h at room temperature in a plate shaker (400 rpm). After three washes with a wash buffer (200 μL/well), the secondary antibody goat antimouse IgG horseradish peroxidase (HRP) conjugated (Thermo Fisher Scientific) was added (100 μL/well) in 1:5000 dilution in the wash buffer. The plates were incubated for 1 h at room temperature in a plate shaker (400 rpm) and washed three times with a wash buffer (200 μL/well). A 1-step ultra TMB-ELISA substrate solution (Thermo Fisher Scientific) was added (50 μL/well), and the color was developed for 8 min in a dark room; 2 N $H_2SO_4$ (50 μL/well) solution was added to stop the reaction. The absorbance was recorded in a Tecan microplate reader at 450 nm.

To determine the IgG subclasses of the anti-HPV16 L2 antibodies, the protocol was followed as described above; however, instead of adding goat antimouse IgG secondary antibody HRP, goat antimouse antibodies specific for IgG2a (Invitrogen, Thermo Fisher Scientific, diluted 1:3000), IgG2b (Invitrogen, Thermo Fisher Scientific, diluted (1:3000)), and IgG1 (Invitrogen, Thermo Fisher Scientific, diluted 1:3000) were added to quantify IgG2a, IgG2b, and IgG1 antibodies, respectively.

To quantify antibodies against Qβ, an ELISA was performed on the VLPs in 96-well MaxiSorp plates (Thermo Fisher Scientific). The plates were coated with 100 μL of 10 μg/mL *Qβ* VLPs per well in PBS (pH = 7.4) and incubated overnight at 4 °C in a shaker. The wells were washed three times with 300 μL of the wash buffer for each wash, and 200 μL of the freshly prepared 2% (v/v) bovine serum albumin (BSA) (Sigma-Aldrich) solution in PBS was added to each well. The plates were incubated for 1 h at room temperature in a plate shaker (400 rpm). The wells were again washed three times using 300 μL of the wash buffer for each wash. A 2-fold serial dilution of mice plasma (diluted in PBS + 1% (w/v) BSA solution) was performed and added to the wells (100 μL/well). After 1 h incubation at room temperature in a plate shaker (400 rpm), the plates were washed three times using a wash buffer (300 μL/well) and the goat antimouse IgG secondary antibody HRP (1:5000 dilution in wash buffer) was added to it (100 μL/well). Again, the plates were incubated for 1 h at room temperature in a plate shaker (400 rpm) and washed three times with a wash buffer (300 μL/well). A 1-step ultra TMB-ELISA substrate solution (50 μL/well) was added, and the color was developed in a dark room for 3 min. The reaction was stopped by adding a solution of 2 N $H_2SO_4$ (50 μL/well). The absorbance was recorded in a Tecan microplate reader at 450 nm. The antibody titers were defined as the reciprocal plasma dilution at which the absorbance exceeded the background value by >0.2 for all of the ELISA tests as described previously.[29]

The recognition of Qβ VLPs from MN extracts (Section 2.5) by anti-Qβ antibodies was determined by performing an ELISA test against Qβ VLPs in an identical way as described above, where the 96-well MaxiSorp plates were coated by the microneedle extract in the first step. Either immunized mice plasma or rabbit anti-Qβ antibodies (custom-made, Pacific Immunology) (1:2000 dilution in PBS + 1% (w/v) BSA solution) followed by the addition of goat antimouse IgG horseradish peroxidase (HRP)-conjugated (Thermo Fisher Scientific) secondary antibody (1:5000 dilution in the wash buffer) or goat antirabbit (Invitrogen) IgG secondary antibody HRP (1:5000 dilution in wash buffer) were used for detection.

### 2.8. Pseudovirus Neutralization Assay.

HPV16 pseudovirus (PsHPV) containing the reporter plasmid pfwB (Addgene #37329) encoding green fluorescent protein (GFP), production, and purification were done as described in our previous study.[29] L2-based neutralization assay[29,36] was carried out with the produced PsHPV. Briefly, the extracellular matrix (ECM) was produced in 96-well plates using MCF10A cells; PsHPV was added, followed by overnight incubation at 37 °C. Then, ECM-PsHPV was removed, and the plasma obtained from the vaccinated mice was added to the 2-fold serial dilution and the growth medium was taken as a control. After 6 h of incubation at 37 °C, pgsa-745 cells were added and the plates were incubated for 48 h. Finally, the infectivity of PsHPV was determined by flow cytometry (BD Accuri C6) by measuring the expression levels of GFP in the infected cells. The neutralization titer was defined as the reciprocal of the highest plasma dilution that inhibited 50% of the infection relative to the control plasma.

### 2.9. Statistical Analysis.

Statistical analysis between groups was performed by unpaired two-tailed Student's *t* test (Microsoft Excel) and plotted using Origin Pro software. $p > 0.05$ was taken as statistically not significant (ns). The values and sample sizes are given in the Section 3 and in the figure legends. The error bars were obtained from the standard deviations of the data sets.

## 3. RESULTS AND DISCUSSION

We optimized the Q$\beta$-based HPV vaccine candidate in a previous study and followed this design,[29] with chemical conjugation of the $L2_{17–31}$ epitope via its C-terminus and a CGGSGGGSG linker (Figure 1A). A two-step method using the $SM(PEG)_8$ cross-linker was used: in the first step, Q$\beta$ was conjugated to $SM(PEG)_8$ by an NHS-ester reaction through the addressable amine groups on the Q$\beta$ surface, and in the second step, the HPV epitope was linked to the $SM(PEG)_8$ through a maleimide reaction. The $L2_{17–31}$ peptide has two internal cysteine residues; thus, we have designed a flexible and unstructured C-terminal linker to ensure that the C-terminal cysteine is the most accessible for conjugation. There is a possibility that Q$\beta$ could attach to the internal cysteine groups when added in excess; however, the resulting immunology indicates successful epitope display. The resulting Q$\beta$-HPV VLPs were characterized by SDS-PAGE, FPLC, TEM, and DLS. The presence of an additional protein band with a molecular weight of ~17 kDa in SDS-PAGE analysis (Figure 1B) indicates successful conjugation of the peptide (molecular weight: ~2.7 kDa) to the Q$\beta$ coat protein (molecular weight: ~14 kDa). The analysis of the band intensity reveals that ~33% of the coat proteins was modified to Q$\beta$-HPV. The FPLC chromatogram (Figure 1C) indicates that VLPs were primarily monodisperse; however, a small population of aggregated particles was detected. TEM micrographs are shown in Figure 1D, further confirming the structural integrity of the Q$\beta$-HPV vaccine candidate. DLS results show Q$\beta$-HPV VLPs with an average diameter of 33 nm; the slight increase in the hydrodynamic diameter compared to unmodified Q$\beta$ VLPs is consistent with epitope surface display. All characterization methods indicate a successful synthesis of high-purity Q$\beta$-HPV VLPs by chemical conjugation and are consistent with our previous reports. Furthermore, a vaccine candidate was also prepared by genetic recombination, but this construct was not

as effective as the conjugated version (lower efficacy was explained by the lower antigen loading achieved by genetic vs chemical display) and significantly more difficult to purify (Supporting Information Figures S3 and S4). Therefore, the methods described throughout only use the chemically conjugated construct.

Q$\beta$-HPV VLPs in DI water were mixed into an aqueous PVP solution (500 mg/mL) and cast into microneedle molds. Molds were centrifuged to ensure complete filling and dried overnight to solidify the needles. A photocurable acrylate backing was then placed over the needle array to improve handling of the patches, leading to patches that were robust and easy to transport. A digital image of the 8 mm × 8 mm microneedle patch is shown in Figure 2A. Each patch contained 10 × 10 needles in an array; each needle had a height of 675 $\mu$m and a square base of 200 $\mu$m in width. The microneedles were characterized by SEM, revealing a uniform array of pyramidal needles with sharp tips (tip width = 1–2 $\mu$m; Figure 2B). PVP was used for its safe and nontoxic profile. A molecular weight of 6–16 kDa was used for the preparation of microneedles in an effort to promote clearance of the dissolved polymer; however, the patches prepared were brittle and prone to cracking/crumbling during demolding and desiccation. PVP (40 kDa) was a suitable candidate in these studies that optimized stability and dissolution. Higher-molecular-weight PVP has shown storage in RES tissues, although PVP is considered neither an irritant nor a sensitizer.[37] The LD50 value for PVP (average 40 kDa) is reported to be higher than 100 g/kg body weight in the animal study for oral administration.[37]

To further assess the stability of VLPs inside the microneedle, we dissolved the microneedle patches and characterized the extract. TEM images (Figure 2C) of the released Q$\beta$-HPV show intact particles with no structural differences when compared to those of freshly prepared Q$\beta$-HPV VLPs. SDS-PAGE analysis further confirmed that the epitope was stably conjugated to Q$\beta$-HPV VLPs, as evidenced by the higher-molecular-weight band at ~17 kDa (Figure 2D). Band intensity analysis revealed an equivalent peptide loading (~33%) before and after microneedle fabrication. It is possible that proteins can be degraded or change conformation during microneedle fabrication; to ensure that carrier conformation remained intact, an in vitro ELISA was performed against the carrier. Q$\beta$-HPV VLPs from the microneedle extract were coated and recognized by anti-Q$\beta$ antibodies. No differences were noted when comparing the extract vs freshly prepared Q$\beta$-HPV VLPs (Figure 2E), therefore indicating successful recognition of the carrier. Together, this data supports that Q$\beta$-HPV retained its original conformation and properties during microneedle fabrication.

To deliver therapeutics, microneedles must penetrate at least ~0.25 mm into the skin to overcome the barrier of the stratum corneum.[14] We tested the penetration of the prepared microneedles ex vivo using porcine skin. For this purpose, AlexaFluor-488 was conjugated to Q$\beta$ VLPs using an NHS-ester reaction. The fluorescently labeled VLPs were characterized by SDS-PAGE, FPLC, TEM, and DLS measurements. The SDS gel (Figure 3A) showed a green fluorescent band at the same position of the Q$\beta$ capsid protein in the Coomassie Brilliant Blue channel, confirming a successful conjugation of AlexaFluor-488; an increase in molecular weight is not detectable due to the low molecular weight of the AlexaFluor-488 label (molecular weight: ~ 0.6 kDa). FPLC (Figure 3B) showed a single peak and elution profile consistent with intact Q$\beta$, with AlexaFluor-488 coeluting with the

Q$\beta$ VLPs. TEM analysis verified intact icosahedral VLPs (Figure 3C). A small increase in the hydrodynamic volume was determined by DLS, with the hydrodynamic diameter of AlexaFluor-488-labeled Q$\beta$ found to be 38 nm (Figure 3D). This result is likely due to a small proportion of low-level assemblies that cannot be resolved by DLS. These Q$\beta$-Alexa VLPs were then loaded into a microneedle patch as described above and applied to porcine skin with a commercial spring applicator. The microneedle dissolved in the skin within 2 min, and ~1 to 2 mm sections were hand-cut with a razor blade and analyzed using fluorescence microscopy. The top-view and cross-sectional images in Figure 3E,F confirmed the presence of the Q$\beta$-Alexa, indicating that the microneedle penetrated the pigskin, with the cargo diffusing to a depth of ~0.75 mm into the skin. These results validate that our microneedles can both dissolve rapidly and deliver their payload deeper than 0.25 mm to pass the skin barrier.

The in vivo efficacy of the Q$\beta$-HPV VLP-loaded microneedle patches was evaluated and compared with traditional hypodermic subcutaneous (SC) injection. The following groups were tested: 100 and 500 $\mu$g Q$\beta$-HPV VLP loaded into microneedle patches vs 1.5 and 100 $\mu$g Q$\beta$-HPV VLP delivered via SC injection. Each group was given two doses (prime and boost) in an interval of 3 weeks. Based on our volumetric estimate (ratio of needle volume to patch volume), we obtain that only 1.5% of VLP could be delivered at most in vivo since most of the vaccine formulations would occupy the backing. Hence, 100 $\mu$g of Q$\beta$-HPV VLP-loaded microneedle patches would deliver only 1.5 $\mu$g of VLP to the mouse and could be compared with 1.5 $\mu$g of dose hypodermic injection group. Future designs, such as a specially designed pressing tool,[38] could address this issue to avoid the majority of the active ingredient being lost as waste material. Injection-molded microneedles could be another alternative to concentrate all VLPs in the tip. Lastly, to assess any immunogenic effects of the polymer material, blank microneedle patches were administered. Microneedles were applied using a spring applicator and remained applied on the skin overnight to allow for the complete dissolution of the microneedles (Figure S5A). The patches took longer to dissolve when applied to mice (overnight); however, we would anticipate a rapid dissolution if translated to the clinic since pig and human skin share similar hydration levels.[39-41]

SEM imaging of the microneedle patches post application confirmed that the microneedle tips were completely dissolved (Figure S5B). Immunological assays followed a prime-boost immunization schedule with two doses 3 weeks apart. Plasma was collected pre- and postimmunization, every 2 weeks post vaccination and continued up to day 50 (Figure 4A). Plasma was analyzed by ELISA against the $L2_{17–31}$ epitope to quantify the anti-HPV16 L2 IgG titer. Data shows that the blank microneedles did not show any antibody response (Figure 4B,C), as expected. The antibody titers sustained their high values from day 18 up to the end of the experiment (day 50) (Figure 4B). As discussed above, 100 $\mu$g of VLP-loaded microneedle patch would deliver at most 1.5 $\mu$g dose intradermally. Comparing this 1.5 $\mu$g intradermal dose with the 1.5 $\mu$g dose administered via subcutaneous injection, we find that the final antibody titer at day 50 was about 6-fold higher for the intradermal dose (Figure 4B,C), showing the vastly improved efficacy of intradermal administration. However, when 500 $\mu$g of VLP-loaded microneedle patch delivering 7.5 $\mu$g dose intradermally (as per volumetric estimate) was administered, the final antibody titer at day 50 increased by only about 24% compared to 100 $\mu$g of VLP-loaded microneedle patch, thus indicating

a saturation effect on the efficacy for intradermal administration (Figure 4B,C). In fact, such a saturation effect on the final antibody titer production was seen for the delivery by subcutaneous injection also. For zero dose delivery, the antibody titer level remains close to zero always and the final titer level at day 50 increases to about $2 \times 10^4$ after administering a 1.5 $\mu$g dose by subcutaneous injection. However, when a 100 $\mu$g dose was administered by subcutaneous injection, the final titer level at day 50 increased to only about $1.4 \times 10^5$ (Figure 4B), thus indicating a saturation effect on the production of antibody titer with higher dose. In the supplementary calculation (see Supporting Information Figure S6 and the Analysis of Dose Sparing Effect section), we provide an approximate formula connecting the final antibody titer production with the microneedle dose by fitting and comparing our data from Figure 4B and give a justification of our volumetric calculation determining the delivery of intradermal dose in our case.

The anti-Q$\beta$ IgG titer was also obtained for each group, as shown in Figure S7, and not surprisingly, all animals developed a carrier-specific immune response. The distribution of different antibody subtypes was evaluated, and all groups were found to have IgG2a/IgG1 < 1 (Figure 4D), indicating a Th2 bias or predominant humoral response as expected from a prophylactic vaccine.

Finally, we determined the efficacy of vaccine candidates to neutralize HPV, using an in vitro HPV pseudovirus neutralization assay.[36] The details of the HPV pseudovirus preparation were described previously.[29,36] In brief, an HPV pseudovirus containing green fluorescent protein (GFP) was produced, and the plasma from immunized mice was used to evaluate neutralization using pgsa-745 cells and flow cytometry, monitoring the GFP channel. The plasma from each group was incubated with HPV pseudovirus in the extracellular matrix that was produced by MCF10A cells. The supernatant was then removed and cultured with pgsa-745 cells. A dilution series of plasma was tested, and the inhibition of infection was quantified by measuring GFP expression (compared to control cells containing HPV pseudovirus only). Reduction of the GFP signal represents a decrease of infected cells, which indicates neutralization capacity of the plasma. The blank microneedle group served as negative control, whereas the mice plasma from the subcutaneously injected group served as the positive control. The PsHPV concentration was adjusted to keep the infection rate of control cells at 50–60% infectivity. The neutralization assay indicates that plasma generated via microneedle administration matched the efficacy of plasma from SC administration of the Q$\beta$-HPV VLP vaccine candidate (Figure 4E). The unpaired two-tailed Student's *t* test revealed that the differences were not statistically significant between different vaccine groups ($p > 0.05$). The dotted line indicates the neutralization titer for each case, where 50% of the cells were infected. In sum, microneedle patches produced antibodies of equivalent neutralization quality, as did those that were generated by traditional subcutaneous injection and at higher titers when compared for available dose.

Lastly, we assessed the shelf-stability of the microneedle HPV vaccine candidate. We sought to determine the shelf-life of unrefrigerated patches. To determine the long-term stability of Q$\beta$-HPV VLPs and the purity of the antigen, microneedles were loaded with VLPs and kept for ~5 months in a desiccator at room temperature. SEM micrographs of a microneedle patch (Figure 5A) demonstrate that the microneedles retain the same tip sharpness as

freshly produced patches. Microneedle patches were dissolved in buffer, and extracts were characterized by TEM, SDS-PAGE, SEM, and ELISA. Results of SDS-PAGE, TEM, and ELISA were consistent with those of freshly produced patches and confirm the structural integrity of Q$\beta$-HPV VLPs (Figure 5B-D). ELISA analysis was completed by coating the place with a microneedle extract diluted 100-fold and evaluated for binding by immunized mice plasma (1:32 000 dilution), where mice had been injected with a single 100 $\mu$g dose of vaccine as a control. In summary, these analyses confirm that Q$\beta$-HPV VLPs are stable at room temperature for at least ~5 months, potentially indicating that our delivery device is free from the requirements of cold-chain transportation and storage.

## 4. CONCLUSIONS

We have demonstrated effective vaccine delivery using shelf-stable, dissolvable microneedle patches containing a Q$\beta$-HPV VLP vaccine formulation. The microneedle-based vaccine showed comparable efficiency to traditional injection-based formulations, and we have demonstrated our method's advantages over current delivery methods. Our results demonstrate that the microneedle delivery system elicits a significantly higher immune response against the HPV16 L2 peptide antigen when controlling for administered dose. A dose sparing effect was observed when antibody titers of effectively equivalent doses (normalized based on the volumetric calculation) administered via microneedle patch vs subcutaneous injections were compared. In future studies, the dose sparing effect could be studied in more detail with more data points.

Previous work has indicated that the self-administration of microneedles has equivalent efficacy as when administered by a health-care professional, opening the door for self-administration to accelerate mass vaccination programs.[17] These microneedles and the encapsulated Q$\beta$-HPV VLP vaccine are stable for at least 5 months at room temperature, eliminating the need for cold-chain distribution. The use of such shelf-stable, self-administered microneedles would decrease the cost of mass vaccination programs drastically, enabling widespread HPV vaccination in both developing and developed countries. Finally, the techniques and formulations of our vaccine candidate and delivery device could be readily adapted to other clinical settings and other infectious diseases. Due to the flexibility and versatility of the Q$\beta$ VLP platform, creating a new self-administrable shelf-stable vaccine may be as easy as selecting a new suitable peptide and conjugating it to a VLP.

## Supplementary Material

Refer to Web version on PubMed Central for supplementary material.

## Funding

RAPID CMMI-2027668 to N.F.S. and J.K.P.; R21AI161306 to N.F.S. and J.K.P.; O.A.O.R. acknowledges the UC MEXUS-CONACYT Postdoctoral Fellowship 2019–2020 number FE-19-58 and 2020–2021 number FE-20-136.

## REFERENCES


(1). Centers for Disease Control and Prevention (CDC), Genital HPV Infection – CDC Fact Sheet *CDC Fact Sheets* 2014, 12.

(2). Garbuglia AR; Lapa D; Sias C; Capobianchi MR; Del Porto P The Use of Both Therapeutic and Prophylactic Vaccines in the Therapy of Papillomavirus Disease. Front. Immunol 2020, 11, No. 188. [PubMed: 32133000]

(3). Whitehead M; Öhlschläger P; Almajhdi FN; Alloza L; Marzábal P; Meyers AE; Hitzeroth II; Rybicki EP Human Papillomavirus (HPV) Type 16 E7 Protein Bodies Cause Tumour Regression in Mice. BMC Cancer 2014, 14, No. 367. [PubMed: 24885328]

(4). Hallez S; Simon P; Maudoux F; Doyen J; Noël JC; Beliard A; Capelle X; Buxant F; Fayt I; Lagrost AC; Hubert P; Gerday C; Burny A; Boniver J; Foidart JM; Delvenne P; Jacobs N Phase I/II Trial of Immunogenicity of a Human Papillomavirus (HPV) Type 16 E7 Protein-Based Vaccine in Women with Oncogenic HPV-Positive Cervical Intraepithelial Neoplasia. Cancer Immunol. Immunother. 2004, 53, 642–650. [PubMed: 14985860]

(5). Petrosky E; Bocchini JA; Hariri S; Chesson H; Curtis CR; Saraiya M; Unger ER; Markowitz LE; Centers for Disease Control and Prevention (CDC). Use of 9-Valent Human Papillomavirus (HPV) Vaccine: Updated HPV Vaccination Recommendations of the Advisory Committee on Immunization Practices. MMWR Morb. Mortal. Wkly. Rep 2015, 64, 300–304. [PubMed: 25811679]

(6). Kirby T FDA Approves New Upgraded Gardasil 9. Lancet Oncol. 2015, 16, No. e56.

(7). Zhai L; Tumban E Gardasil-9: A Global Survey of Projected Efficacy. Antiviral Res. 2016, 130, 101–109. [PubMed: 27040313]

(8). Walker TY; Elam-Evans LD; Yankey D; Markowitz LE; Williams CL; Fredua B; Singleton JA; Stokley S National, Regional, State, and Selected Local Area Vaccination Coverage Among Adolescents Aged 13–17 Years – United States, 2018. MMWR Morb. Mortal. Wkly. Rep 2019, 68, 718–723. [PubMed: 31437143]

(9). Wigle J; Fontenot HB; Zimet GD Global Delivery of Human Papillomavirus Vaccines. Pediatr. Clin. North Am 2016, 63, 81–95. [PubMed: 26613690]

(10). Reagan-Steiner S; Yankey D; Jeyarajah J; Elam-Evans LD; Singleton JA; Curtis CR; MacNeil J; Markowitz LE; Stokley S National, Regional, State, and Selected Local Area Vaccination Coverage Among Adolescents Aged 13–17 Years — United States, 2014. MMWR Morb. Mortal. Wkly. Rep 2015, 64, 784–792. [PubMed: 26225476]

(11). Stokley S; Jeyarajah J; Yankey D; Cano M; Gee J; Roark J; Curtis RC; Markowitz L In Immunization Services Division, National Center for Immunization and Respiratory Diseases, CDC;Centers for Disease Control and Prevention (CDC). Human Papillomavirus Vaccination Coverage among Adolescents, 2007–2013, and Postlicensure Vaccine Safety Monitoring, 2006–2014, United States. Morb. Mortal. Wkly. Rep, 2014; pp 620–624.

(12). Arya J; Prausnitz MR Microneedle Patches for Vaccination in Developing Countries. J. Controlled Release 2016, 240, 135–141.

(13). Sharma S; Hatware K; Bhadane P; Sindhikar S; Mishra DK Recent Advances in Microneedle Composites for Biomedical Applications: Advanced Drug Delivery Technologies. Mater. Sci. Eng., C 2019, 103, No. 109717.

(14). Prausnitz MR Engineering Microneedle Patches for Vaccination and Drug Delivery to Skin. Annu. Rev. Chem. Biomol. Eng 2017, 8, 177–200. [PubMed: 28375775]

(15). Zaric M; Lyubomska O; Poux C; Hanna ML; McCrudden MT; Malissen B; Ingram RJ; Power UF; Scott CJ; Donnelly RF; Kissenpfennig A Dissolving Microneedle Delivery of Nanoparticle-Encapsulated Antigen Elicits Efficient Cross-Priming and Th1 Immune Responses by Murine Langerhans Cells. J. Invest. Dermatol 2015, 135, 425–434. [PubMed: 25243789]

(16). Zaric M; Lyubomska O; Touzelet O; Poux C; Al-Zahrani S; Fay F; Wallace L; Terhorst D; Malissen B; Henri S; Power UF; Scott CJ; Donnelly RF; Kissenpfennig A Skin Dendritic Cell Targeting via Microneedle Arrays Laden with Antigen-Encapsulated Poly- D, l -Lactide- Co -Glycolide Nanoparticles Induces Efficient Antitumor and Antiviral Immune Responses. ACS Nano 2013, 7, 2042–2055. [PubMed: 23373658]

(17). Norman JJ; Arya JM; McClain MA; Frew PM; Meltzer MI; Prausnitz MR Microneedle Patches: Usability and Acceptability for Self-Vaccination against Influenza. Vaccine 2014, 32, 1856–1862. [PubMed: 24530146]

(18). Bachmann MF; Jennings GT Vaccine Delivery: A Matter of Size, Geometry, Kinetics and Molecular Patterns. Nat. Rev. Immunol 2010, 10, 787–796. [PubMed: 20948547]

(19). Chackerian B Virus-like Particles: Flexible Platforms for Vaccine Development. Expert Rev. Vaccines 2007, 6, 381–390. [PubMed: 17542753]

(20). Chung YH; Cai H; Steinmetz NF Viral Nanoparticles for Drug Delivery, Imaging, Immunotherapy, and Theranostic Applications. Adv. Drug Delivery Rev 2020, 156, 214–235.

(21). Pokorski JK; Steinmetz NF The Art of Engineering Viral Nanoparticles. Mol. Pharmaceutics 2011, 8, 29–43.

(22). Frietze KM; Peabody DS; Chackerian B Engineering Virus-like Particles as Vaccine Platforms. Curr. Opin. Virol 2016, 18, 44–49. [PubMed: 27039982]

(23). Patel KG; Swartz JR Surface Functionalization of Virus-like Particles by Direct Conjugation Using Azide-Alkyne Click Chemistry. Bioconjugate Chem. 2011, 22, 376–387.

(24). Prasuhn DE; Singh P; Strable E; Brown S; Manchester M; Finn MG Plasma Clearance of Bacteriophage Q$\beta$ Particles as a Function of Surface Charge. J. Am. Chem. Soc 2008, 130, 1328–1334. [PubMed: 18177041]

(25). Lee PW; Shukla S; Wallat JD; Danda C; Steinmetz NF; Maia J; Pokorski JK Biodegradable Viral Nanoparticle/Polymer Implants Prepared via Melt-Processing. ACS Nano 2017, 11, 8777–8789. [PubMed: 28902491]

(26). Golmohammadi R; Fridborg K; Bundule M; Valegård K; Liljas L The Crystal Structure of Bacteriophage Q$\beta$ at 3.5 Å Resolution. Structure 1996, 4, 543–554. [PubMed: 8736553]

(27). Tyler M; Tumban E; Chackerian B Second-Generation Prophylactic HPV Vaccines: Successes and Challenges. Expert Rev. Vaccines 2014, 13, 247–255. [PubMed: 24350614]

(28). Trus BL; Buck CB; Cheng N; Lowy DR; Steven AC; Schiller JT Localization of the HPV-16 Minor Capsid Protein L2 by Difference Imaging. Microsc. Microanal 2005, 11, 642–643.

(29). Shao S; Ortega-Rivera OA; Ray S; Pokorski JK; Steinmetz NF A Scalable Manufacturing Approach to Single Dose Vaccination against Hpv. Vaccines 2021, 9, No. 66. [PubMed: 33478147]

(30). Zhai L; Peabody J; Pang YYS; Schiller J; Chackerian B; Tumban E A Novel Candidate HPV Vaccine: MS2 Phage VLP Displaying a Tandem HPV L2 Peptide Offers Similar Protection in Mice to Gardasil-9. Antiviral Res. 2017, 147, 116–123. [PubMed: 28939477]

(31). Tumban E; Peabody J; Peabody DS; Chackerian B A Pan-HPV Vaccine Based on Bacteriophage PP7 VLPs Displaying Broadly Cross-Neutralizing Epitopes from the HPV Minor Capsid Protein, L2. PLoS One 2011, 6, No. e23310. [PubMed: 21858066]

(32). Tyler M; Tumban E; Dziduszko A; Ozbun MA; Peabody DS; Chackerian B Immunization with a Consensus Epitope from Human Papillomavirus L2 Induces Antibodies That Are Broadly Neutralizing. Vaccine 2014, 32, 4267–4274. [PubMed: 24962748]

(33). Brown SD; Fiedler JD; Finn MG Assembly of Hybrid Bacteriophage Q$\beta$ Virus-like Particles. Biochemistry 2009, 48, 11155–11157. [PubMed: 19848414]

(34). Ortega-Rivera OA; Pokorski JK; Steinmetz NF A Single-Dose, Implant-Based, Trivalent Virus-like Particle Vaccine against “Cholesterol Checkpoint” Proteins. Adv. Ther 2021, 4, No. 2100014.

(35). Ortega-Rivera OA; Shin MD; Chen A; Beiss V; Moreno-Gonzalez MA; Lopez-Ramirez MA; Reynoso M; Wang H; Hurst BL; Wang J; Pokorski JK; Steinmetz NF Trivalent Subunit Vaccine Candidates for COVID-19 and Their Delivery Devices. J. Am. Chem. Soc 2021, 143, 14748–14765. [PubMed: 34490778]

(36). Day PM; Pang YYS; Kines RC; Thompson CD; Lowy DR; Schiller JT A Human Papillomavirus (HPV) in Vitro Neutralization Assay That Recapitulates the in Vitro Process of Infection Provides a Sensitive Measure of HPV L2 Infection-Inhibiting Antibodies. Clin. Vaccine Immunol 2012, 19, 1075–1082. [PubMed: 22593236]

(37). Kurakula M; Rao GSNK Pharmaceutical Assessment of Polyvinylpyrrolidone (PVP): As Excipient from Conventional to Controlled Delivery Systems with a Spotlight on COVID-19 Inhibition. J. Drug Delivery Sci. Technol 2020, 60, No. 102046.

(38). Chiu YH; Chen MC; Wan SW Sodium Hyaluronate/Chitosan Composite Microneedles as a Single-Dose Intradermal Immunization System. Biomacromolecules 2018, 19, 2278–2285. [PubMed: 29722966]

(39). Li S; Zheng X; Nie Y; Chen W; Liu Z; Tao Y; Hu X; Hu Y; Qiao H; Qi Q; Pei Q; Cai D; Yu M; Mou C Defining Key Genes Regulating Morphogenesis of Apocrine Sweat Gland in Sheepskin. Front. Genet 2019, 9, No. 739. [PubMed: 30761184]

(40). Summerfield A; Meurens F; Ricklin ME The Immunology of the Porcine Skin and Its Value as a Model for Human Skin. Mol. Immunol 2015, 66, 14–21. [PubMed: 25466611]

(41). Wei JCJ; Edwards GA; Martin DJ; Huang H; Crichton ML; Kendall MAF Allometric Scaling of Skin Thickness, Elasticity, Viscoelasticity to Mass for Micro-Medical Device Translation: From Mice, Rats, Rabbits, Pigs to Humans. Sci. Rep 2017, 7, No. 15885. [PubMed: 29162871]

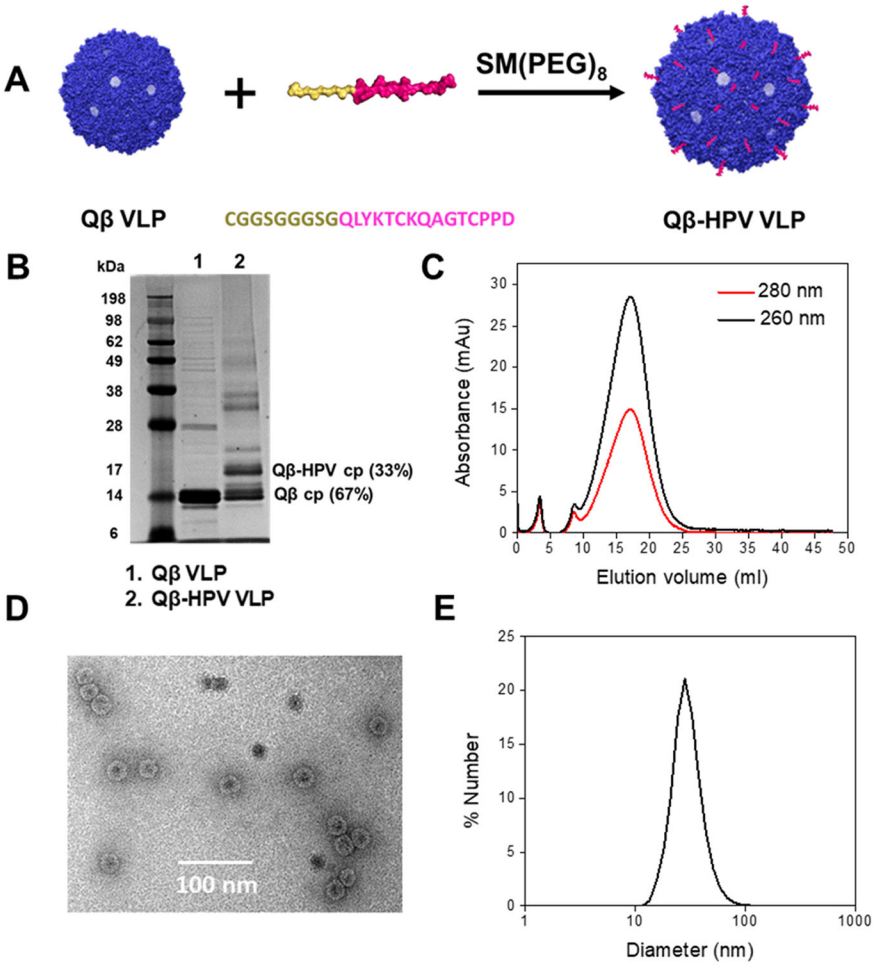


**Figure 1.**

Preparation and characterization of VLPs. (A) Chemical conjugation scheme of Q$\beta$ VLP with the HPV epitope $L2_{17–31}$. Characterization of Q$\beta$-HPV VLP after conjugation: (B) sodium dodecyl sulfate-polyacrylamide gel electrophoresis (SDS-PAGE) gel for both Q$\beta$ VLP and Q$\beta$-HPV VLP, (C) fast protein liquid chromatography (FPLC), (D) transmission electron microscopic (TEM) images of UAc (2% w/v)-stained Q$\beta$-HPV VLPs, and (E) DLS, where Q$\beta$-HPV VLPs show 33 nm and PDI = 0.266.

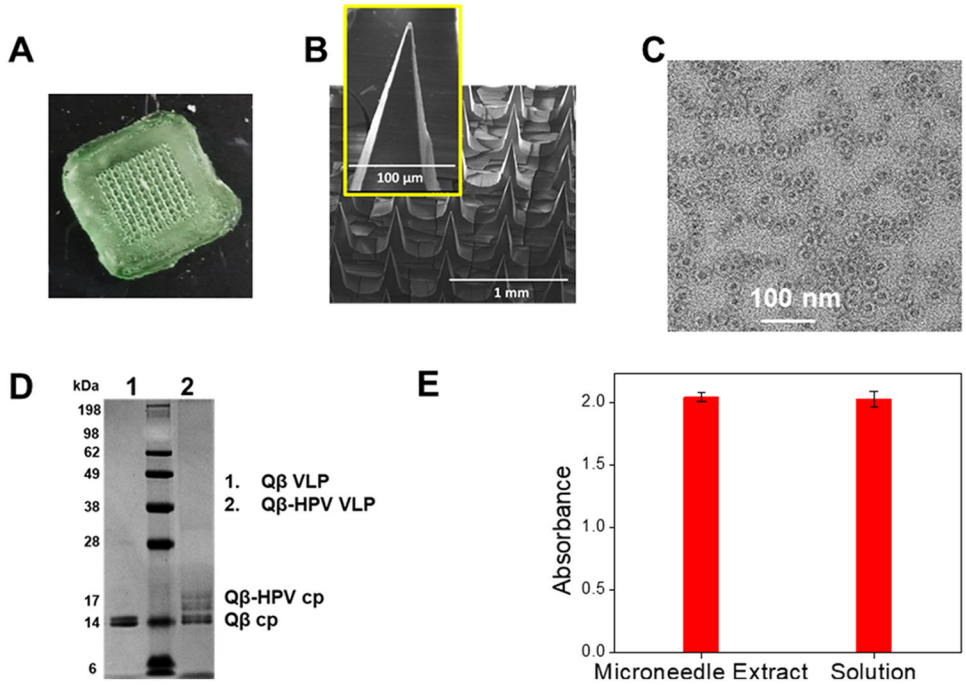


**Figure 2.**

Characterization of microneedles and microneedle extract: (A) representative digital image of the microneedle patch (8 mm × 8 mm). (B) SEM images of the microneedles; the inset shows a microneedle tip. (C) TEM images of the microneedle extract show uniform and intact Q$\beta$-HPV VLPs. (D) SDS-PAGE gel, where the microneedle extract with Q$\beta$-HPV VLPs (lane 2) was run and compared with the unmodified Q$\beta$ VLP (lane 1). (E) Absorbance at 450 nm after ELISA against Q$\beta$ comparing Q$\beta$-HPV from the microneedle extracts vs freshly prepared (solution).

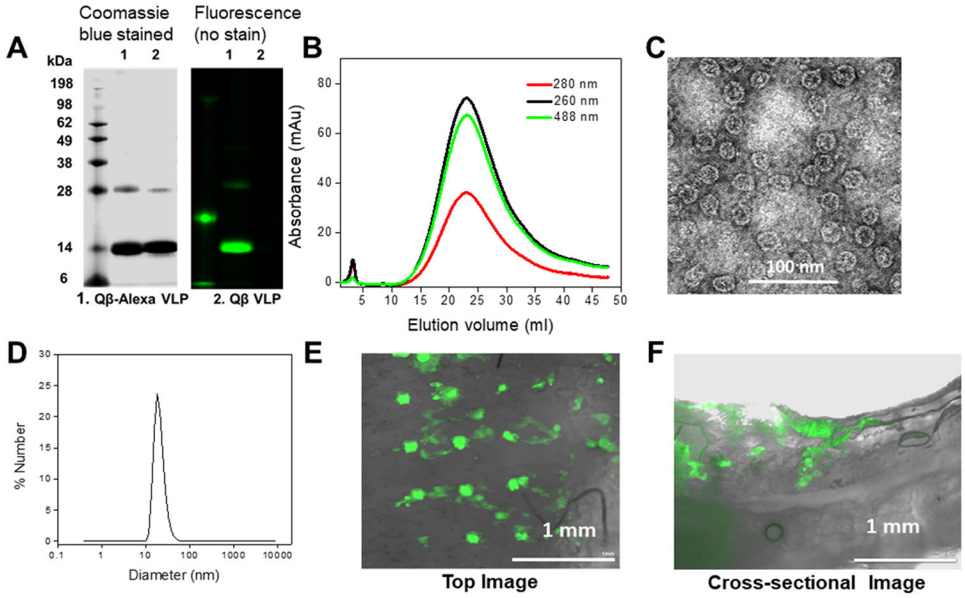


**Figure 3.**

Pigskin penetration assay and characterization of Q$\beta$ labeled with AlexaFluor-488 (A) SDS-PAGE gel of Q$\beta$-Alexa (lane 1) vs Q$\beta$ VLPs (lane 2). The gels were imaged under UV light (right panel) and bright light after Coomassie staining (left panel). (B) FPLC of Q$\beta$-Alexa. (C) TEM images of Q$\beta$-Alexa (stained with 2% (w/v) UAc). (d) DLS of Q$\beta$-Alexa, demonstrating a diameter of 38 nm, PDI: 0.025. (E, F) The top-view and cross-sectional images taken after a 2 min insertion of the Q$\beta$-Alexa VLP-loaded microneedle patch into pigskin; images were taken using a fluorescence microscope.

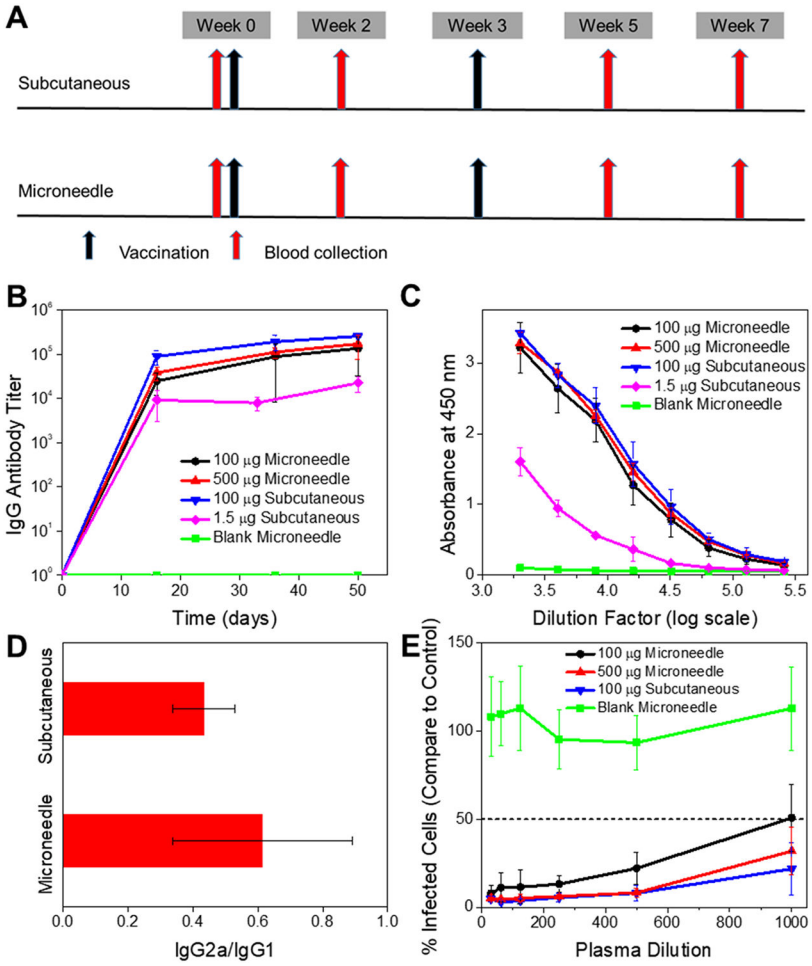


**Figure 4.**

Immunization by microneedle patches. Groups of mice were immunized with Q$\beta$-HPV with varying doses and delivery methods; 100 $\mu$g by microneedle, 500 $\mu$g by microneedle, 100 $\mu$g by subcutaneous injection, and 1.5 $\mu$g by subcutaneous injection. (A) Immunization and bleeding schedule. Mice were immunized twice, 3 weeks apart, and blood was collected every 2 weeks after each dose, until day 50. (B) Time course of antibody titer against HPV16 L2 peptide for different groups. (C) Absorbance values at 450 nm in ELISA test for different dilutions after 2 weeks of the second dose for $n = 3$ mice from each group. (D) Antibody subtyping between microneedle delivery and subcutaneous injection. (E) Pseudovirus neutralization data. The percentage of the infected cells was given relative to the control cells, which were not exposed to plasma. The crossing point of the dotted line (50% infectivity compared to the control) with the neutralization curve corresponded to the neutralization titer. The neutralization titer was above 1000 for all formulations. The unpaired two-tailed Student's $t$ test between different groups with the HPV vaccine formulations (100 $\mu$g microneedle, 500 $\mu$g microneedle, 100 $\mu$g subcutaneous) has shown $p > 0.05$ (ns) between each other, indicating they are statistically not different. Each of the vaccine group has shown $p < 0.05$ with the blank microneedle.

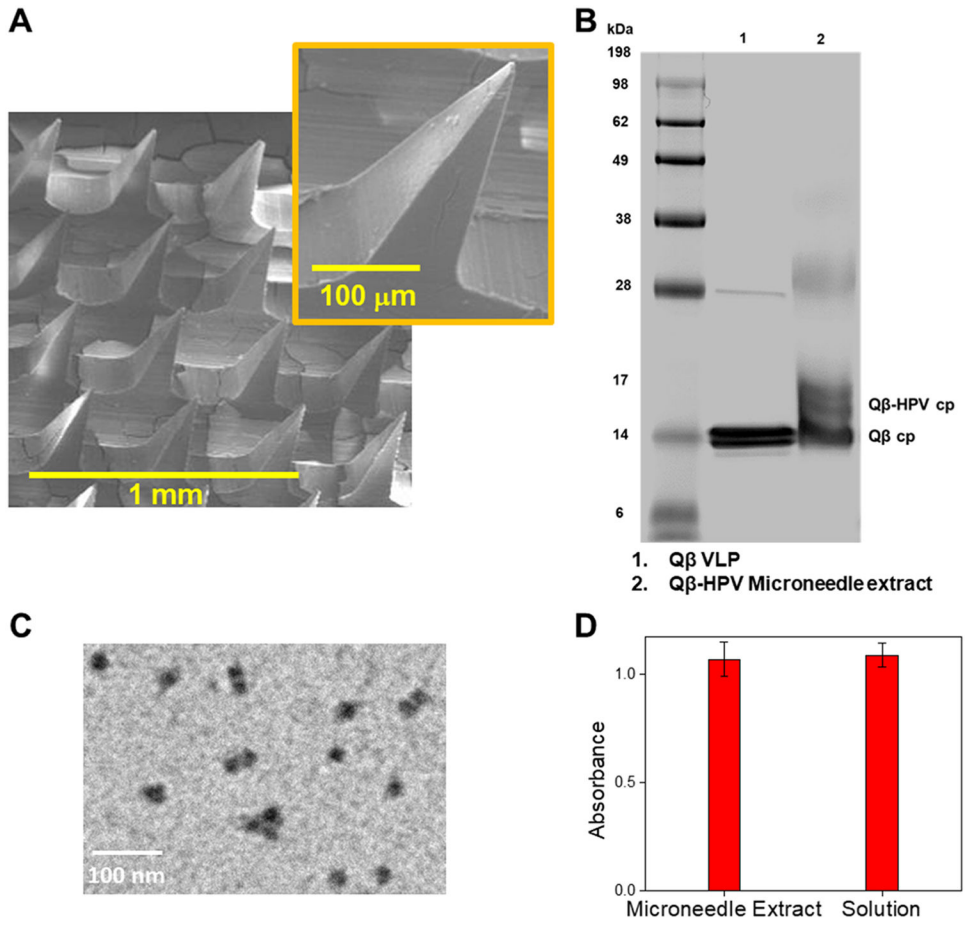


**Figure 5.**

Characterization of Q$\beta$-HPV VLPs after a long-term storage (5 months) at room temperature: (A) SEM images of the microneedle patch; the inset gives a closer look to the tip. (B) SDS-PAGE of the microneedle extract carrying Q$\beta$-HPV VLPs and compared with Q$\beta$ VLPs as control. (C) TEM images of Q$\beta$-HPV VLPs. (D) Absorbance at 450 nm after running an ELISA test of the obtained microneedle extract against immunized mice plasma to compare the efficiency of the antigen to recognize cognate antibody; pure Q$\beta$ VLP solution was used as a control.